**REVIEW**

# Temporal and photon number resolution of superconducting nanowire single-photon detectors

Jun Xie[1] · Hengbin Zhang[2]

## Abstract

Single-photon detectors based on superconducting nanowires (SNSPDs) are promising technologies with good comprehensive performance, especially their excellent temporal resolution for applications in quantum precision measurements and time-varying ultimate detection. The response time of an SNSPD can be characterized by aspects of hotspot thermal relaxation and electrical relaxation, which are also responsible for the time jitter of the SNSPD. The factors affecting the temporal resolution of an SNSPD, the underlying physical mechanism, the intrinsic limit, and possible optimization methods are reviewed. The poor energy resolution and lack of photon number resolution for conventional SNSPDs can be overcome by using high-impedance readouts, novel device structures, characterization methods and, most importantly, SNSPD arrays, which can simultaneously further improve the temporal resolution. The study of the temporal and photon number resolution of SNSPDs helps reveal the underlying physics and is valuable for their new application in various practical engineering areas.

## 1 Introduction

Superconducting nanowire single-photon detectors (SNSPDs) are among the most popular detectors for detecting single photons with visible to near-infrared (VIS–NIR) wavelengths. Due to their ultrahigh timing accuracy, quantum efficiency, ultralow dark count rates, and so on, the application fields of SNSPDs have expanded from incipient quantum communication and laser ranging to practically all territories of ultimate-sensitivity photon detection. At present, the superconducting materials used for the micro/nanofabrication of SNSPDs include Nb [1, 2], NbN [3, 4], NbTiN [5, 6], TaN [7, 8], MoSi [9, 10], WSi [11–13], etc., all of which are typy-II superconductors, whose magnetic flux vortex and photon-generated quasiparticles significantly affect or even determine the detection process. The photon detection mechanism and its influence on the detector performance make SNSPDs more promising and deserving of further in-depth study. This review is organized as follows: In Sect. 2, the various time-related processes in an

SNSPD are discussed, aiming to shed light on the mechanism responsible for the temporal resolution. The factors influencing the time jitter are elaborated from four aspects—photon wavelength, nanowire device, dimensionality effect, and quantum-related fluctuations—which indicate or imply the ultimate limit and improvement directions of the time jitter. In Sect. 3, the potential for the energy and photon number resolution of SNSPDs is detailed from the perspectives of high-impedance readouts, novel device structures, characterization methods, and detector array architectures. The photon number resolution capability with a high temporal resolution of SNSPDs opens new areas never previously attained by traditional single-photon detectors.

## 2 Temporal resolution of SNSPDs

The temporal resolution of the single photon detector is determined by the characterization of every single component that leads to inaccuracy due to a timing jitter caused by finite slope and bandwidth limitations [14]. For the readout signals, this resolution corresponds to identifying the voltage pulse packets induced by different photons. For an SNSPD, the temporal resolution is generally the same as the time jitter and is influenced by thermal and electrical processes. The thermal processes, including photon absorption by nanowires, hot spot generation, and hot spot diffusion, are related

✉ Hengbin Zhang
zhanghengbin826@163.com

1 Qian Xuesen Laboratory of Space Technology,
Beijing 100094, China

2 China Academy of Space Technology, Beijing 100094, China

to the evolution of quasiparticles in nanowires. The duration of the thermal processes can be indirectly obtained via two-photon pump rate curve measurements [15, 16] or reluctance measurements [12]. Due to the ultrathin and ultranarrow structure of nanowires and the effect of electrothermal negative feedback, the time scale of the thermal cycle is only tens of picoseconds [17]. The electrical response time refers to the entire process from a photon being incident to output of electrical pulses when treating nanowires as part of a distributed electrical circuit [18]. The large kinetic inductance of nanowires increases the electrical response time to approximately 10 ns [19, 20]. As shown in Fig. 1, the rising edge of the response signal is much faster than the falling edge.

## 2.1 Time-related processes in SNSPDs

The temporal resolution is an overwhelming advantage of SNSPDs, which benefit from many intrinsic physical processes. As shown in Fig. 1, the time-interval-related parameters mainly include $T_d$ (time delay in the formation of resistance states after a photon is incident), $T_T$ (thermal cycle time), and $T_E$ (electrical response time). The other time-related parameters include $t_{th}$ (thermal time of electrons), $t_l$ (time latency), $t_t$ (trigger time), $t_s$ (rise time of thermal processes), $t_{ri}$ (rise time of electrical processes), $t_{rl}$ (fall time of thermal processes), and $t_f$ (fall time of electrical processes).

Vodolazov et al. systematically calculated the factors influencing $T_d$ in SNSPDs, including the photon incident position, nanowire width, and bias current, using a combination of the 2-T model and the time-dependent Ginzburg–Landau (TDGL) method [21, 22]. In addition, factors that optimize the performance parameters of SNSPDs, such as the time jitter, were analysed, and the thermalization time of electrons ($t_s$) and the relaxation time of hot spots ($t_{rl}$) were semiquantitatively estimated by defining the

electron–phonon coupling coefficient ($\gamma$). The combination of solved equations includes the TDGL equation, the thermal diffusion equation, and the full current conservation equation, which provide the superconducting order parameters, temperature of a quasiparticle, and potential distribution of the thermal processes, respectively, as well as the equivalent circuit equation, which describes the electrical processes.

By ignoring the complicated microphysical processes, single-photon detection can be simply described by a one-dimensional (1D) thermal diffusion equation and an equivalent circuit equation [23], where the nanowire can be equivalent to a resistance and an inductance, and the process from photon absorption to output of an electrical pulse can be simulated. The output pulse waveform is mainly composed of a time delay, a rising edge, and a falling edge (Fig. 1). The rise time ($t_{ri}$) is the duration of the nanowire transition from the superconducting state to the resistive state, which is generally expressed as $t_{ri} = L_k/(50\Omega + R_n)$ (where $L_k$ and $R_n$ are the kinetic inductance and load resistance of the nanowire, respectively) [19]. The fall time ($t_f$) is the transition time for the opposite process and is expressed as $t_f = L_k/(50\Omega)$. $t_f$ is also commonly referred to as the reset or relaxation time. Therefore, for the SNSPD readout obtained with the traditional circuit structure, $t_f$ is mainly restricted by the $L_k$ of the superconducting nanowire.

## 2.2 Time jitter

The factors influencing the time jitter for SNSPDs are complex. The external parameters include the bias current, temperature [24, 25], etc. For the test system, the signal-to-noise ratio, bias mode [26, 27], readout circuit [28–31], synchronization signal, and jitter of the laser [32] all affect the time jitter test result. With the rapid development of

**Fig. 1** Schematic of the time-related processes and parameters in SNSPDs and the references to physical parameters, which are described in the following. (the scale bar of the X-axis for thermal process and electrical process are different)
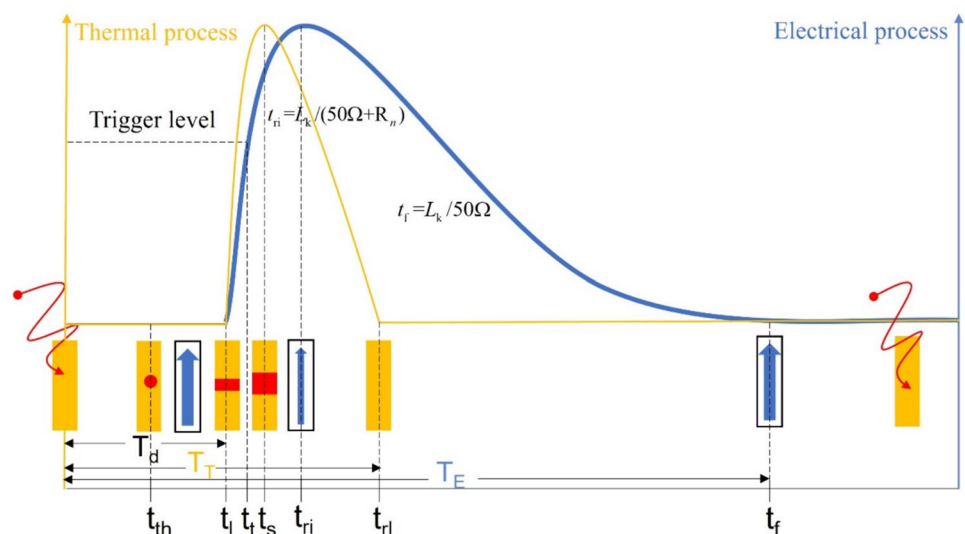
quantum communication and laser ranging, research on time jitter has deeply examined the internal physical mechanism because of the urgent need for ultrahigh time measurement accuracy. As shown in Fig. 2, some numerical calculations showed that the theoretical limit of the time jitter is less than 1 ps [33], which is still much lower than the lowest value of 7.7 ps measured for meander nanowires [34] and lower than the value of 2.6 ps measured for a special single-nanowire structure [35]. Therefore, to further improve the timing accuracy, a more systematic study of the influencing factors and optimization methods of the intrinsic time jitter must be conducted. The factors influencing the intrinsic jitter can be mainly divided into the photon wavelength, nanowire device, dimensionality effect, and quantum-related fluctuations, which further include the cross-section effect, delay line effect, superconductor material, spatial distribution inhomogeneity, Fano fluctuations, and quantum jitter.

### 2.2.1 Photon wavelength

For VIS–NIR wavelengths, such as photons with wavelengths of 800 nm and 1560 nm, when the same test method and working parameters are adopted, the difference in the time jitter caused solely by the photon wavelength is only a few picoseconds [36], so this difference was often ignored in early studies of SNSPDs [37]. The relationship between the time jitter and photon wavelength was recently tested using a single 5 µm-long NbN device combined with a low-temperature RF amplifier. Korzh et al. found that the time



jitter gradually decreased with increasing photon energy, and when the largest bias current was applied, the time jitter was 2.6 ps, 3.0 ps, and 4.3 ps for 532 nm, 775 nm, and 1550 nm wavelength photons, respectively [35]. The difference gradually increased with decreasing bias current, which was explained by the transition of the detection regime from single-photon to multiphoton detection (the criterion was $j_{sw} = j(w_e/(w_e - d_{ns}))$, where $j_{sw}$, $j$, $w_e$ and $d_{ns}$ represent the sidewalk critical current density, bias current density, effective stripe width, and diameter of the hotspot for single-photon absorption, respectively) [38]. Related theoretical research has shown a similar trend. The TDGL equation for the initial phase of resistive hot spot generation was solved phenomenologically [39] and microscopically [40]. Considering the spatial distribution inhomogeneity and Fano fluctuations from the perspective of the delay time, the relationships of the time jitter with the photon wavelength and bias current were well explained (Fig. 3).

Currently, the vast majority of SNSPD research and applications involve VIS–NIR wavelengths. Although the use of SNSPDs in time-of-flight mass spectrometry (TOF–MS) has been expanded to detect keV polymers [41–43], latching tends to occur in the detection of photons at this energy, which severely restricts the imposed bias current [2, 7, 44, 45]. Preliminary studies indicate that X-ray SNSPDs have ultrahigh photon count rates, lower dark counts, and a similar time performance (Table 1) compared with SNSPDs working at VIS–NIR wavelengths. Notably, the photon detection mechanism of X-ray SNSPDs is not solely the photoelectric effect, and the influence of the Compton effect cannot be ignored. However, its specific influence requires further theoretical and experimental research for clarification.

We first characterized the time jitter performance of X-ray SNSPDs [46, 47]. Through the key technologies of a high-aspect-ratio superconducting nanowire device preparation system, an anti-latching active quenching bias readout circuit, and a continuously stable 0.3 ps pulsed laser−plasma X-ray source, the time jitter of X-ray SNSPDs was obtained and continuously optimized. We systematically investigated the influence of different parameters, such as the nanowire width, detection area, bias current and photon energy (Table 1). The minimal FWHM time jitter was 15 ps for a 250 nm wide nanowire, a $20 \times 20$ µm$^2$ detection area, and a 800 µm total length device. Notably, there were no events outside the Gaussian or quasi-Gaussian time-resolved correlation distribution, which indicated that no substrate-mediated secondary detection events occurred in the X-ray SNSPDs [48].

The ultralow time jitter performance of SNSPDs was also expanded to mid-infrared single-photon detection. By replacing the commonly used InSb detector with SNSPDs, Chen et al. obtained a 3.7 ns time jitter under mid-infrared laser-induced fluorescence for molecular science. As
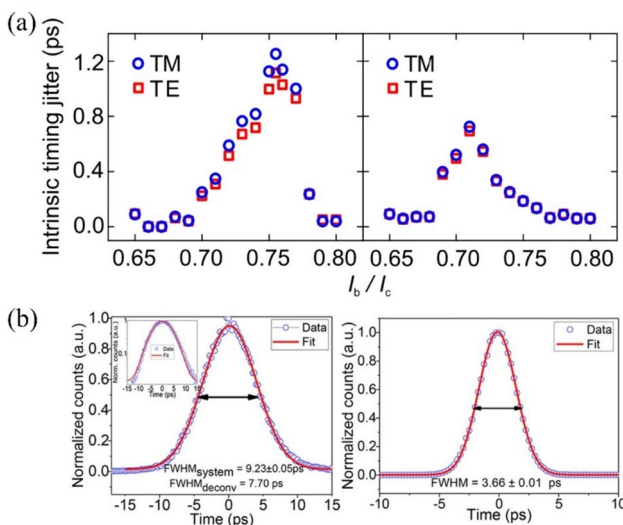
**Fig. 2** **a** Simulations of time jitter induced by vortex crossing with varying bias current for 100 nm- and 50 nm-wide nanowires. Reprinted from [33], with the permission of AIP Publishing. **b** Results of the jitter measurements under single-photon fluxes and higher photon fluxes. Adapted from [34], Copyright © 2020 American Chemical Society, CC-BY-NC-ND

**Fig. 3** Statistical histograms of the delay time as a function of bias current for photon wavelengths of 800 nm (**a**) and 1560 nm (**b**). Reprinted figure with permission from [36]. Copyright 2017 by the American Physical Society
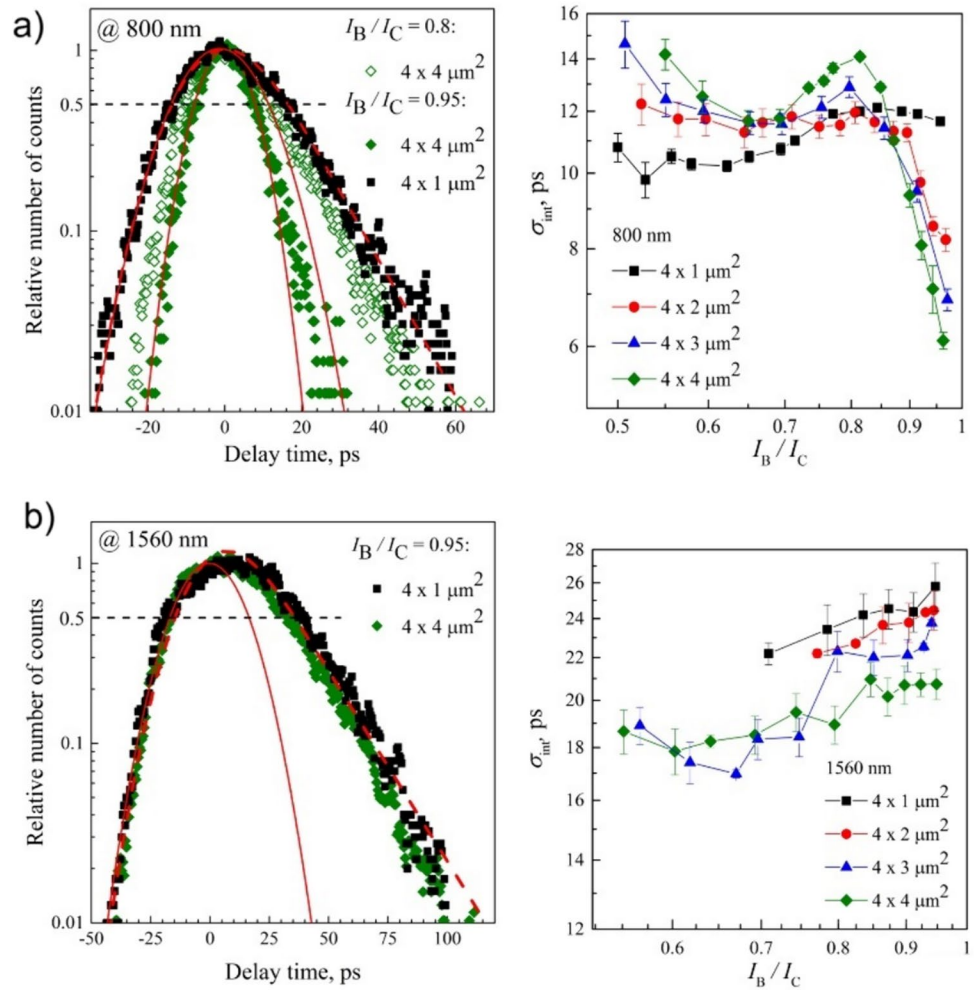


**Table 1** Geometry, switching current and minimal time jitter for X-ray SNSPDs[47]

| Detectors | | Total length (µm) | Switching current (µA) | Minimal timing jitter (ps) |
|---|---|---|---|---|
| Various areas with 250-nm-wide nanowires | $10 \times 10$ µm$^2$ | 200 | 2012 | 15.0 |
| | $20 \times 20$ µm$^2$ | 800 | 1962 | 17.9 |
| | $50 \times 50$ µm$^2$ | 5000 | 1800 | 20.1 |
| | $100 \times 100$ µm$^2$ | 20,000 | 1600 | 39.7 |
| Various widths with a $50 \times 50$ µm$^2$ area | 150 nm | 8333 | 900 | 28.5 |
| | 250 nm | 5000 | 1800 | 21.9 |
| | 350 nm | 3571 | 2500 | 25.2 |
| | 450 nm | 2778 | 3500 | 24.2 |

shown in Fig. 4, the prominent deterioration of the time jitter compared with that on the order of 100 ps based on near-infrared femtosecond laser pulses is thought to be induced by the much longer mid-infrared laser pulse duration[49]. Recently, the time jitter of the NbTiN SNSPD

response to single photons with different mid-infrared wavelengths was systematically investigated; the FWHM jitter ranged from 13.2 to 30.3 ps for photon wavelengths ranging from 1.56 to 3.5 µm, and simultaneously, > 70% system detection efficiency was realized [6, 50].
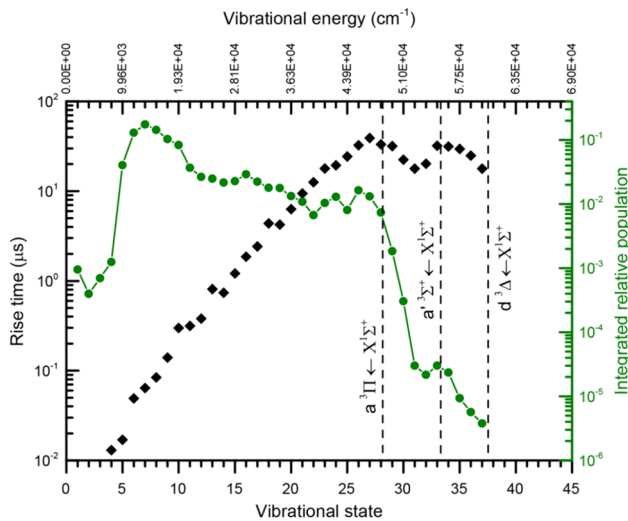
**Fig. 4** Molecular vibrational-state-dependent rise time (black diamonds), which is defined as the peak time of the dispersed fluorescence temporal profile, and time-integrated vibrational population (solid line). Reprinted with permission from [49]. Copyright 2017 American Chemical Society

### 2.2.2 Superconducting materials

The nanowire-device-induced time jitter mainly involves superconducting materials and spatial inhomogeneity. The incipiently used and continuously developed superconducting materials for SNSPDs are primarily niobium-series superconductors, such as NbN [35, 51, 52], NbTiN [53, 54], and NbRe [55]. The intrinsic time jitter of meander nanowires fabricated from these superconducting films is approximately 20 ps, and the lowest value to date is 2.6 ps when using a 5 μm-long straight single nanowire and a silicon germanium cryogenic amplifier [35]. The measured time jitter of SNSPDs fabricated from a Nb single material is 110 ps [56], which is significantly greater than that for the Nb compounds. This difference is ascribed to the slower thermalization of the quasiparticles in Nb than in NbN. The slightly later emerging amorphous tungsten and molybdenum series of superconductors, such as WSi, MoSi [9, 11, 57, 58], and $Mo_{0.75}Ge_{0.25}$ [59], have a time jitter of approximately 70 ps. The lowest time jitter obtained to date is 6 ps, which is approximately two times larger than that of the niobium series superconductors and was also measured for a 5 μm-long single nanowire and a silicon germanium cryogenic low-noise amplifier (LNA). The larger time jitter of amorphous superconductor-based SNSPDs may be induced by the uncertain disordered state of the materials. Other candidate superconducting materials for photon detection are high-Tc superconductors. Recent work on $YBa_2Cu_3O_{7-\delta}$ (YBCO)-based superconducting microwire photon detectors has indicated that the

time jitter is 100 ps at the lowest, which is significantly greater than that of low-Tc superconductor SNSPDs [60].

Currently, the typical Ginzburg–Landau (GL) coherence length of the abovementioned superconductors for the fabrication of SNSPDs is only approximately 5 nm, which is much smaller than the conventional nanowire width of 100 nm. Even when the operating temperature increases to 0.9 times the superconducting transition temperature, the coherence length is only on the order of 10 nm [47]. Some theoretical analyses predicted that the ideal material for fabricating SNSPDs is a type II "dirty" superconductor with a low electron mobility ($D \approx 0.5 cm^2/s$), where the absorbed photon energy localized in a small range of hot spots rapidly increases the temperature of hot electrons and thus improves the detection sensitivity. However, there are no reports in the literature on SNSPDs using type I superconductors with coherence lengths comparable to the nanowire width. Previous experiments and theoretical analyses of SNSPDs [49, 50] have shown that if photodetectors that meet the conditions of 1D superconductors can be fabricated, then their unique low-dimensional quantum characteristics may lead to new detection mechanisms and break through the performance bottlenecks of current SNSPDs.

For type I superconductors such as tin (Sn), indium (In), and lead (Pb) with very large coherence lengths (> 300 nm), their fabricated SNSPDs can easily meet the "Likharev limit" ($W \leq 4.4\xi(T)$, where $W$ is the nanowire width and $\xi(T)$ is the coherence length) [61–63]. Therefore, even if there is an external magnetic field, theoretically, the flux vortex cannot enter the superconductor. For 1D superconducting nanowires with very large coherence lengths, the boundary flux tunnelling barrier significantly increases, and the probability of thermally excited phase slip significantly decreases in the common operation temperature range [64, 65](Fig. 5); thus, the device is expected to have a lower dark count. The latest experiments showed that magnetic flux tunnelling is one of the main factors causing uncertainty in the photon arrival time when the time jitter is within the order of 10 ps [33], and the ultrafast intrinsic transformation time of 1D superconductor phase slip may significantly inhibit the intrinsic time jitter of an SNSPD.

In addition, one of the fundamental limitations restricting further decreases in the time jitter of SNSPDs is that the superconducting critical current ($I_C^{max}$) is far from the decoupling current ($I_{dep}$), and the supercurrent compression coefficient R ($I_c^{max}/I_{dep}$) can only reach 0.3 [66]. In general, the larger the bias current is, the better the comprehensive performance of the SNSPD device [67–69]. The reasons are as follows: First, the nonuniformity of the nanowire width caused by corners or impurity defects will

**Fig. 5** Current−voltage (I−V) characteristics of a NbN nanowire. **a** I−V curves at 200 mK. **b** Temperature dependence of current-biased I−V curves. **c** Magnetic field dependence of voltage-biased I−V curves. **d** Zoomed-in view near $I_c$ of the voltage-biased I−V curve at 4.2 K. Reprinted with permission from [65]. Copyright 2012 by the American Chemical Society
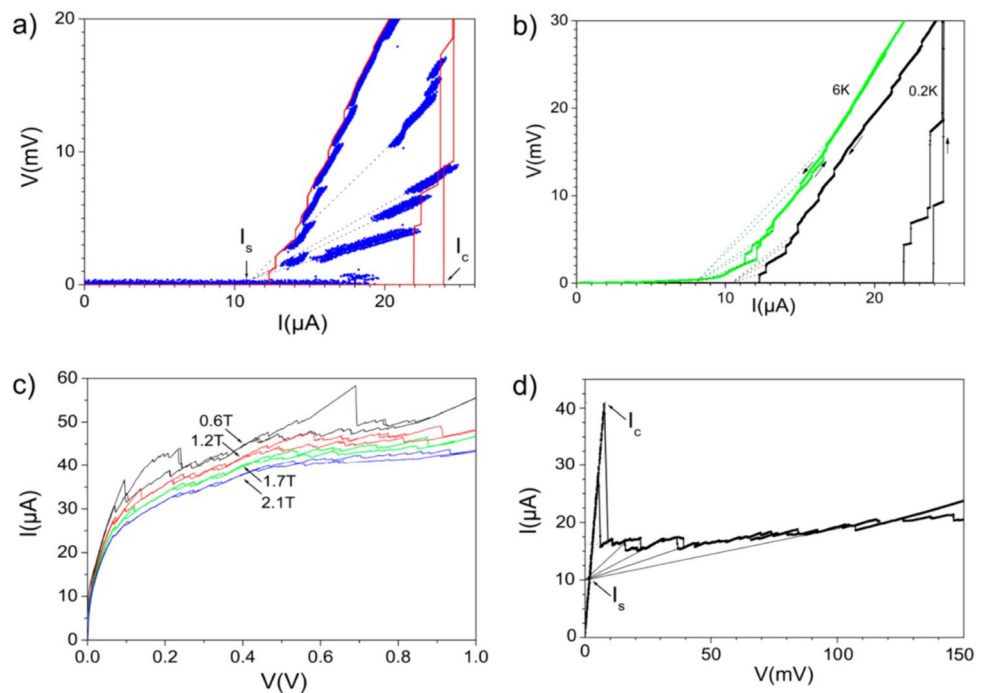
lead to supercurrent compression [70, 71], and differences in parameters such as the corner shape and curvature will also have a significant impact on R [67]. Second, for a type II superconductor that does not meet the "Likharev limit", its superconducting critical current is basically restricted by the pinning current ($I_{pin}$), and its value is only approximately half that of $I_{dep}$ [65, 72]. If the SNSPD device is fabricated from a type I superconductor, then there is no condition for the formation of resistance states such as magnetic flux crossing and vortex pinning, and the superconducting order parameters and other characteristics will not significantly change within the nanowire cross-section. Therefore, the superconducting critical current is mainly limited by the current-carrying capability of the Cooper pair and the bias current that can be applied, approaching the decoupling current. Therefore, the performance indices of SNSPDs, including the time jitter, can be further improved.

Spatial inhomogeneities, such as defects or compression, are another source of material-induced intrinsic time jitter. For example, large fluctuations in the detection efficiency [73, 74] and nonuniform (typically sub-100 nm scale [75]) or disorderly fluctuations in the electronic states will lead to random variations in the critical temperature along the nanowire [76], which results in uncertainty in the photoelectric response of the nanowire. O'Connor et al. demonstrated that the compressed state generated during device fabrication can cause a time jitter of up to 20 ps between the highest and lowest sensitivity locations of the nanowire [77]. Hu et al. simulated random electronic state-induced fluctuations

in the time jitter based on an electrothermal model and the Monte Carlo method [78] and found that distributed inhomogeneities contribute the vast majority of the total sub-15 ps time jitter. Some experiments have also shown that the intrinsic time jitter of wider nanowires is mainly determined by the inhomogeneity of the spatial distribution, while the time jitter of narrow nanowires is mainly determined by Fano fluctuations [79]; however, this result might be induced by the lower impact of spatial inhomogeneities for narrow nanowires than for wider nanowires.

### 2.2.3 Dimensionality effect

The dimensionality effect is also related to the nanowire device, but its origin and influence are significantly different and can be further divided into three dimensions. The time jitter associated with the delay line effect is along the nanowire dimensionality (longitudinal) direction. When superconducting nanowires are treated as transmission lines, the time jitter of photons incident at different longitudinal positions of the nanowires cannot be ignored. Studies have shown that when the size of SNSPD devices increases from $3 \times 3$ to $20 \times 20$ μm$^2$, the delay time caused by the transmission line increases from a few picoseconds to approximately 50 ps [77], although this jitter can be significantly suppressed by using a differential readout circuit [80], it is impossible to overcome entirely due to the inhomogeneity between the high- and low-sensitivity parts of the device. In addition, the response processes of the corner part and straight part of the nanowire are different, and their effects on time jitter

are also different. The highest detection sensitivity occurs at the centre of the nanowire, which is far from the twists and turns [81, 82].

Another dimension is across the nanowire (Y axis), which is often neglected in traditional 1D hot belt models [23]. This dimensionality effect is caused by the uncertainty in the photon incident position within the cross-section of the nanowire. Compared with those incident at the nanowire centre, the photons incident at the edge of the nanowire produce a smaller hot spot and hence a higher electron cloud temperature, resulting in a steeper rising edge of the response pulse [83]. From the perspective of the microcosmic physical mechanism, when photons are incident at different locations across a nanowire, the time delay caused by vortex crossing is different [33]. Therefore, the dimensionality-effect-induced time jitter along the cross section is related to the bias current and nanowire width,

To our knowledge, the dimensionality effect along the nanowire thickness direction (Z axis) has never been investigated for SNSPDs. In an ordinary nanowire device, because the thickness of the nanowire is much smaller than the length and width, the evolution of hot spots and photogenerated quasiparticles along the thickness direction is thought to be instantaneously completed, and the detection model is generally simplified to a 1D or quasi-2D model. Some recent studies have indicated that the thermal transport of superconducting nanowires is affected by their thickness and surfaces [84]. The thermal boundary conductance along the Z axis between the nanowire and the substrate may significantly influence time-related performance metrics such as the maximum count rate, latency, and time jitter. Therefore, the abovementioned thicker superconducting nanowires used for high-energy photon detection or type-II ultralong-coherence-length superconducting materials could provide favourable conditions for studying this unexplored field.

### 2.2.4 Quantum-related fluctuations

Fano fluctuation is a form of quantum-related fluctuations caused by different energy dissipation branches and is

thought to fundamentally limit the spectral resolution and signal-to-noise ratio of superconducting detectors such as superconducting tunnel junction detectors (STJs), superconducting transition edge sensors (TESs) and microwave kinetic-inductance detectors (MKIDs) [85–87]. The nonlinear photon energy-bias current relationship in MoSi SNSPDs in the 750–2050 nm wavelength range was considered evidence of the existence of Fano fluctuations [88]. Moreover, because the thickness of the SNSPD superconducting film is small compared with the mean free path of phonons, the SNSPD is more significantly affected by Fano fluctuations than other superconducting detectors. Kozorezov et al. systematically studied the Fano fluctuations in an SNSPD for the first time and found that Fano fluctuations and spatial distribution inhomogeneity are the key factors for the time jitter to enter the subpicosecond regime. Theoretical calculations showed that the effect of Fano fluctuations can be weakened by increasing the thickness of the superconducting film to reduce the relaxation of high-frequency phonons to the substrate [39].

In addition, Yang et al. of Purdue University proved that theoretically, the minimum time jitter is the relaxation time of the superconducting order parameter when the bias current approaches the critical current, which is called quantum jitter. They believe that if the photon incident position can be accurately measured, then the device structure- and position-dependent time jitter can be completely overcome; however, according to Markov theory, for single-photon detection, the rising edge and falling edge of the output response voltage pulse are not deterministic, as in traditional photodetectors, but rather probabilistic (Fig. 6) [89]. This quantum jitter can be minimized by reducing the temperature, increasing the bias current, increasing the photon energy, or decreasing the line width [90], but it is difficult to overcome fundamentally.

Importantly, the different time-related parameters are inseparable. For example, the rise time and time jitter of SNSPDs are directly associated, and the time jitter of SNSPDs can be conveniently predicted by capturing only the rise time of a single detector pulse [91]. Although the specific value of the time jitter cannot be accurately obtained,



**Fig. 6** Quantum jitter-related vortex crossing rate (**a**) and probability (**b**). Reprinted from [90], with the permission of AIP Publishing
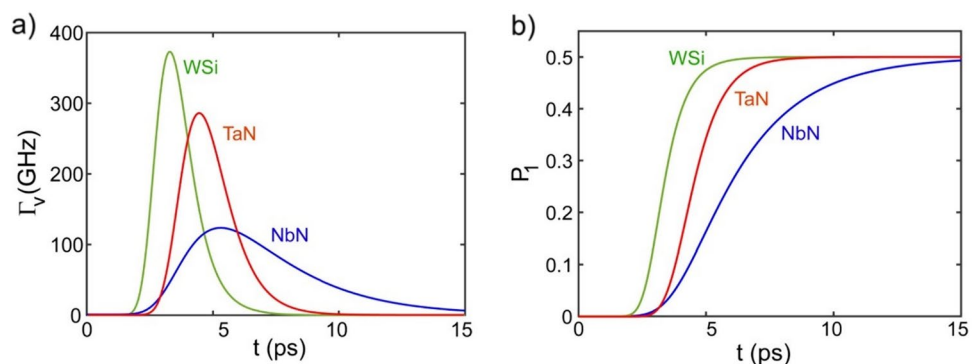
the trend of the time jitter under different conditions can be directly judged, and by designing reference pulses with a known time jitter, the time jitter interval of a single response pulse can be roughly estimated, avoiding the need for many repeated measurements to obtain a statistical histogram. In addition, the count rate and the time jitter have a trade-off relationship [92]. By adopting a linear array of straight superconducting nanowires, Craiciu et al. proved that this tradeoff can be weakened by implementing an independent readout for each element and using a temporal walk correction technique [93]. Moreover, by introducing a correlation calibration method, the time delay of a detection event can be associated with the time interval between the response pulses so that the tradeoff between the time jitter and count rate can be largely eliminated in the software [94]. Therefore, these methods will further enhance the significant advantages of SNSPDs in terms of time-related performance (Table 2).

## 3 Photon number resolution (PNR)

For an ordinary readout circuit of SNSPDs, the amplitude of the response electrical pulse can be described as $V_{pulse} = G \times I_b \times 50\Omega$, where $G$ is the gain of the microwave amplifier and $I_b$ is the bias current of the device. Therefore, unless special device structures [99] or readout circuits [100–103] are employed, most ordinary SNSPD systems cannot directly distinguish incident photons of different energies. The height and width of the voltage pulses for nanowires in response to photons of all wavelengths are identical. Other calibration methods can indirectly enable energy resolution of SNSPDs by utilizing intermediate physical parameters, such as the quantum efficiency [104–106], critical current [107] and arrival time histogram [25]. However, these schemes increase not only the complexity of the test but also the measurement of intermediate parameters,

which still has uncertainties and errors. One exception is the detection of high-energy photons. Owing to the comparable resistance to that of the 50 Ω shunt resistor for μm-wide superconducting nanowires, the pulse amplitude varies with the energy of X-ray photons (Fig. 7), thus providing a direct energy resolution ability of X-ray SNSPDs [2, 7, 8].

### 3.1 Impedance matching

Initially, the loss of photon number resolvability for the ordinary readout circuit of SNSPDs was caused by the impedance mismatch between the nanowire device and the readout circuit. The solutions can be divided into two directions, namely, enhancing the impedance of the readout circuit or decreasing the impedance of the nanowire device, and the former method is more generally adopted. Bell et al. first investigated the impedance of the readout circuitry required for PNR of SNSPDs via electromagnetic simulation. The results of the photon number-dependent signal amplitude
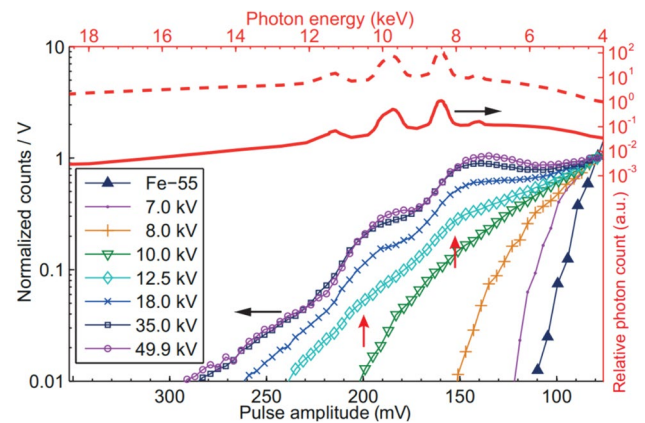
**Fig. 7** X-ray photon energy-dependent amplitude of the response electrical pulse. Reprinted from[2], with the permission of AIP Publishing

**Table 2** The comparison of low time jitter SNSPDs experiments(1550nm wavelength photon)

| Year | Authors | Material | Detector area | Time jitter(ps) |
|------|---------|----------|---------------|-----------------|
| 2004 | Korneev A, et al. [52] | NbN | $10 \times 10\mu m^2$ | < 18 |
| 2005 | Pearlman A, et al. [83] | NbN | $10 \times 10\mu m^2$ | < 18 |
| 2013 | You L, et al. [95] | NbN | $15 \times 15\mu m^2$ | < 18 |
| 2016 | Calandri N, et al. [96] | NbN | $3 \times 3\mu m^2$ | 12 |
| 2016 | Shcheslavskiy, V., et al. [14] | NbN | $7 \times 7\mu m^2$ | 17.8 |
| 2017 | Sidorova M, et al. [36] | NbN | $4 \times 4\mu m^2$ | 13 |
| 2017 | Wu J, et al. [97] | NbN | $10 \times 10\mu m^2$ | 11.9 |
| 2018 | Sidorova M, et al. [81] | NbN | $40\mu m$ (straight) | 9.2 |
| 2018 | Sidorova M, et al. [98] | NbN | $40\mu m$ (straight) | 7.7 |
| 2019 | Caloz M, et al. [58] | MoSi | $5\mu m$ (straight) | 10.6 |
| 2020 | Esmaeil Zadeh I, et al. [34] | NbTiN | $25 \times 25\mu m^2$ | 7.7 |
| 2020 | Korzh B, et al. [35] | NbN | $5\mu m$ (straight) | 4.3 |

confirmed that the greater the impedance matching is, the greater the number of photons that can be resolved [108]. However, the length of the transmission lines connecting the device and the readout circuit must be severely restricted to eliminate the effects of standard 50 Ω coaxial transmission lines. In addition, single flux quantum (SFQ) logic circuits are suitable for SNSPD readout with PNR [109–112]. Simulations and verification experiments demonstrated the advantages of a wide band, low noise, low-power dissipation, and greater photon resolvability for the SFQ or deuteronic MMD2Q and DFQA readout methods. Impedance matching can also be implemented on the nanowire device side. Zhu et al. demonstrated an impedance-matching nanowire device based on a gradually varied taper transmission line; the starting width of the taper was 500 nm [113]. This tapered structure brings about PNR with better time-related properties (higher pulse amplitude and smaller time jitter) and avoids complex nanofabrication or the use of a special readout circuit.

Recently, some studies have indicated that the inherent rise time of the response signal reflects the number of absorbed photons when converted into a statistical amplitude, which can be decoded under the initial SNSPD structure by a cryogenic LNA and converting differentiating circuits [114–116]. The shoulders of the Poisson statistics peak amplitude histogram correspond to the different photon numbers. To explain this detector behaviour, Nicolic et al. developed a universal model for the turn-on dynamics of SNSPDs to more fundamentally describe the rising edge of the detection process [117, 118], other than the macroscopic expression mentioned in Sect. 2.1. In recent work on heralded single-photon source (HSPS) characterization, specialized cryogenic LNAs could be dispensable, and photon number information could be obtained from only the rising edge of the output signal [119].

### 3.2 Novel device structures and characterization methods

Some novel nanowire device structures have also been proposed to solve the challenge of PNR of SNSPDs. Smith designed a new three-layer architecture that puts the electric leads beneath the nanowires, similar to a charge-coupled device (CCD), which allows very large-scale array integration. However, due to the complexity of the device structure and fabrication process, no test results for prototype devices have been reported. The unique feature of the new device is its ability to simultaneously measure the photon number and spatial resolution. Recently, Zou et al. integrated the superconducting nanowire current reservoir structure with yTron and resolved the photon number with high fidelity by reading the format of the supercurrent stored in the current reservoir. Moreover, the number of photons incident on

SNSPDs can be determined by adopting new characterization methods. For example, by using the positive operator valued measure (POVM) method, the low-photon-number regime can be reconstructed, and the extracted mean photon number parameters of a bright state can be obtained [120]. In addition, the photon number can be quickly and efficiently resolved through complete and uniform coherent absorption in distributed SNSPD arrays, and the single-photon mode avoids complicated spatial or temporal multiplexing [121]. Very recently, researches proposed a new promising PNR method of SNSPD based on the photon statistics, which could resolve up to 7 photons with high efficiencies (around 94.5% at 940 nm) and high timing resolution (18.4 ps at 1064 nm) [122].

### 3.3 Detector array architectures

Single-photon detectors with PNR are core devices in quantum information processing and related fields [123–128]. The most direct and effective PNR ability is achieved through the independent readout of traditional SNSPDs by a multichannel. Dauler et al. first fabricated and tested a two-element independently biased SNSPD, and a 44 ps FWHM coincidence time jitter and a fourfold increase in the maximum counting rate were realized by decreasing the kinetic inductance per element [129]. Liu et al. combined the power of the response signal of four channels with different voltage pulse heights to determine the photon number information, which fit the theoretical calculations of the Poisson distribution very well [130]. To avoid the current crowding effect from the bends of nanowires, Zhang et al. proposed circular interleaved nanowire arrays, for which the total maximum count rate reached 0.93 GHz and exceeded 1.5 GHz with up to 9 and 16 photons resolvable, respectively [131, 132]. Based on the time-to-digital converter (TDC) in a field-programmable gate array (FPGA), photon counting was also realized in multichannel superconducting nanowires with a time jitter below 22 ps (RMS) and 2.5 mW power consumption [133]. The use ratio of the FPGA device was only 2.7%, which indicates the large photon-number resolvability for extension. However, the multiple independent readouts of each channel result in complex circuit modules, such as current bias source, amplifier, and bias-T modules, which become impractical as the number of channels gradually increases. In addition, the frequency division multiplexing scheme for SNSPDs learned from MKIDs is promising to overcome this challenge [134–136] and deserve in-depth further investigation systematically.

In other device architectures, the nanowires and bias resistors are arranged in parallel or series. Compared with multichannel arrays, these approaches adopt a much smaller readout channel and thus have more scalability. Korneev et al. first proposed a multisection nanowire meander

connected in parallel. Theoretically, the equivalent inductance of N parallel connected nanowires is $N^2$ times smaller than that of single meander nanowires with equal areas, and consequently, the count rate is $N^2$ times larger. The photon response waveform amplitudes scale with the mean number of m photons per pulse [137–139], and m can even extend to 20 ~ 30, which bridges the gap between conventional avalanche single-photon detectors and integral linear photon diodes [140, 141]. To explore the PNR mechanism of such a detector structure, Marsili et al. developed the electrical and optical equivalents of parallel nanowire detectors (PNDs) and proposed a more stable device structure with a bias resistor ($R_0$) serially connected to each section of nanowires to ensure an effective tradeoff between the response speed and quantum efficiency [142]. However, $R_0$ cannot be increased to above approximately 100 Ω; otherwise, the device tends to latch, which limits the PNR ability to 4–6 and the efficiency to a few percent [128]. Owing to the PNDs, the fidelity of the detector can be characterized, and the full $P_{nm}$ matrix can be used to reconstruct the statistics of HSPSs [143, 144].

To overcome the current redistribution problem of PNDs, Jahanmirinejad et al. developed series nanowire detectors (SNDs) based on N-series connected superconducting nanowires, each connected in parallel to an integrated resistor [145–148]. The relationships of both the voltage signal amplitude and the count rate with the incident light power proved the photon-number resolvability of the SNDs [149]. Although the system efficiency was as low as ~ 0.17% due to the inhomogeneity problem originating from the large active area of the device, it could be immediately enhanced by integrating a microcavity or an optical waveguide [150, 151]. Compared with PNDs, SNDs are more promising because of their large photon number scalability, good linearity, and high quantum efficiency [152], as verified by electrothermal simulation of the influence of several important design parameters.

Notably, the PNR capability of the spatial array SNSPD architectures is not absolute PNR. When two photons are incident on the same parallel wire section, they cannot be resolved at all. The more parallel wires there are, the lower the probability of two photons being absorbed by the same wire section, and the closer we are to true PNR.

In fact, the temporal resolution and PNR of SNSPD arrays can be simultaneously improved. Using PNDs, Goltsman et al. obtained the N-fold relationship between the waveform voltage amplitude and the photon number N, and the fall time of the response signal obeyed the $1/N^2$ law [153]. Although the time jitter of the device is not directly characterized, as analysed in Sect. 2.1, the time jitter is an overall direct ratio related to the fall time or rise time of the voltage pulse. Dauler et al. demonstrated that four-element photon-number-resolved SNSPDs have a sub-30 ps precision arrival time for single photons, which is very promising for characterizing continuous light sources, and have a high count rate for fast photon-counting applications [154]. Most theoretical and experimental fidelity research has indicated that the use of only four elements is the best choice. In addition, based on the combination of the abovementioned SND and PND structures, Miki et al. and Cheng et al. exploited the avalanche of PNDs (and renamed them SNAP) and proposed the series-M-SNAP (M and N correspond to the number of series and parallel connected nanowires, respectively) [155, 156]. This variant achieved a $1/n^2$ reduction in the reset time and an n-fold improvement in the signal-to-noise ratio compared to those of standard SNSPDs, which could accelerate its usage in a range of novel applications. Soon afterwards, by adding a short terminator to the DC port of a bias-T, Tao et al. decreased the pulse width from 25 to 1 ns for six-pixel fibre-coupled SNDs, which also demonstrated the fast counting rate and low time jitter PNR capability of the SND device structure [150].

Then, Perrenoud et al. further improved the device structure. By integrating wider large unexposed nanowires into traditional PNDs, the current was redistributed among the nanowires, which prevented crosstalk between parallel nanowires and thus realized latch-free operation up to 200 MHz using a single coaxial line [157]. Recently, a 100-pixel spatiotemporal multiplexed SNSPD array was designed by Cheng et al. that could resolve up to 100 photons [158]. The fast rising edge of the detector response signal was a high-frequency readout from an 80 nm-wide NbN nanowire in series and an 800 nm wire-width on-chip NbN delay line, while the low-frequency reset loop of the detector falling edge signal was realized by an on-chip 400 nm wire-width NbN meander inductance and a 5 μm wire-width, 50 μm-long Cr/Au resistance, which avoided latching of the detector and prevented direct crosstalk of each pixel. This scheme simultaneously realized high PNR, fast detector response, and precise spatial resolution in the same nanowire device. Finally, Resta et al. simply and efficiently expanded SNSPD arrays to 14 independent pixels, achieving a detection efficiency of 90% at a 1.5 GHz count rate, and the fidelities for two and three photons were 74% and 57%, respectively [159]. Due to their ultrahigh count rate, multielement SNSPDs are a unique solution for high-speed photon number quantum communication and imaging (Table 3).

## 4 Conclusion

In summary, high temporal resolution is an overwhelming advantage of SNSPDs, and the array device structure can realize PNR without adopting complex readout circuit. The ultrahigh temporal resolution with a moderate PNR will undoubtedly make superconducting nanowires irreplaceable

**Table 3** The experiments of PNR ability of SNSPDs

| Authors | Method | Photon number resolvable | Time jitter(ps) |
| --- | --- | --- | --- |
| Dauler E. A, et al. [129] | multichannel | 2 | 44 |
| Jahanmirinejad S, et al. [146] | SND | 4 | 80 |
| Zhou ZL, et al. [149] | SND | 12 | 89 |
| Dauler EA, et al. [154] | PND | 4 | 30 |
| Liu DK, et al. [130] | multichannel | 4 | – |
| Lusardi N, et al. [133] | Multichannel + TDC | 4 | 22 |
| Huang J, et al. [131] | multichannel | 9 | 24.9 |
| Ota K, et al. [109] | SFQ | 6 | – |
| Wan C, et al.[110] | BiCMOS | 10 | – |
| Myoren H, et al. [111] | SFQ | 6 | – |
| Cheng RS, et al. [158] | arrays | 100 | 50–90 |
| Resta GV, et al. [159] | arrays | 14 | 21 |

single-photon detectors in some fields, such as high-speed heralded single-photon source characterization and quantum lidar measurement.

**Author contributions** J.X. provided the idea, H.Z. collected the literature and wrote the original draft, J.X. proposed the revision suggestions, H.Z. revised the manuscript.

**Data availability** No datasets were generated or analysed during the current study.

## Declarations

**Conflict of interest** The authors declare no conflicts of interest.

## References

1. A.J. Annunziata et al., Reset dynamics and latching in niobium superconducting nanowire single-photon detectors. J. Appl. Phys. (2010). https://doi.org/10.1063/1.3498809
2. K. Inderbitzin et al., An ultra-fast superconducting Nb nanowire single-photon detector for soft x-rays. Appl. Phys. Lett. **101**, 162601 (2012)
3. G.N. Gol'tsman et al., Picosecond superconducting single-photon optical detector. Appl. Phys. Lett. **79**, 705–707 (2001)
4. X.Y. Zhang et al., NbN Superconducting nanowire single-photon detector with 90 5% saturated system detection efficiency and 14.7 ps System Jitter at 1550 nm Wavelength. IEEE J. Select. Top. Quant. Electron **28**, 1–8 (2022)
5. S. Miki et al., Superconducting NbTiN nanowire single photon detectors with low kinetic inductance. Appl. Phys. Express **2**, 075002 (2009)
6. G.G. Taylor et al., Mid-infrared timing jitter of superconducting nanowire single-photon detectors. Appl. Phys. Lett. (2022). https://doi.org/10.1063/5.0128129
7. K. Inderbitzin, Soft X-Ray single-photon detection with superconducting tantalum nitride and niobium nanowires. IEEE Trans. Appl. Supercond. (2012). https://doi.org/10.1109/TASC.2012.2234496
8. C. Yang et al., Large-area TaN superconducting microwire single photon detectors for X-ray detection. Opt. Express **29**, 21400–21408 (2021)
9. Y.P. Korneeva et al., Superconducting single-photon detector made of MoSi film. Supercond. Sci. Technol. **27**, 095012 (2014)
10. I. Charaev et al., Large-area microwire MoSi single-photon detectors at 1550 nm wavelength. Appl. Phys. Lett. **116**, 242603 (2020)
11. V.B. Verma et al., High-efficiency superconducting nanowire single-photon detectors fabricated from MoSi thin-films. Opt. Express **23**, 33792–33801 (2015)
12. X. Zhang et al., Superconducting fluctuations and characteristic time scales in amorphous WSi. Phys. Rev. B (2018). https://doi.org/10.1103/PhysRevB.97.174502
13. M.S. Allman et al., A near-infrared 64-pixel superconducting nanowire single photon detector array with integrated multiplexed readout. Appl. Phys. Lett. (2015). https://doi.org/10.1063/1.4921318
14. V. Shcheslavskiy et al., Ultrafast time measurements by time-correlated single photon counting coupled with superconducting single photon detector. Rev. Sci. Instrum. (2016). https://doi.org/10.1063/1.4948920
15. F. Marsili et al., Hotspot relaxation dynamics in a current-carrying superconductor. Phys. Rev. B (2016). https://doi.org/10.1103/PhysRevB.93.094518
16. S. Ferrari et al., Hot-spot relaxation time current dependence in niobium nitride waveguide-integrated superconducting nanowire single-photon detectors. Opt. Express **25**, 8739–8750 (2017)
17. K.S. Il'in et al., Picosecond hot-electron energy relaxation in NbN superconducting photodetectors. Appl. Phys. Lett. **76**, 2752–2754 (2000)
18. Q.Y. Zhao, D.F. Santavicca, D. Zhu, B. Noble, K.K. Berggren, A distributed electrical model for superconducting nanowire single photon detectors. Appl. Phys. Lett. (2018). https://doi.org/10.1063/1.5040150
19. A.J. Kerman et al., Kinetic-inductance-limited reset time of superconducting nanowire photon counters. Appl. Phys. Lett. (2006). https://doi.org/10.1063/1.2183810
20. Y.-H. He et al., Statistical analysis of the temporal single-photon response of superconducting nanowire single photon detection. Chin. Phys. B **24**, 060303 (2015)

21. A.N. Zotova, D.Y. Vodolazov, Photon detection by current-carrying superconducting film: a time-dependent Ginzburg-Landau approach. Phys. Rev. B (2012). https://doi.org/10.1103/PhysRevB.85.024509

22. D.Y. Vodolazov, Minimal timing jitter in superconducting nanowire single-photon petectors. Phys. Rev. Appl. (2019). https://doi.org/10.1103/PhysRevApplied.11.014016

23. J.K.W. Yang et al., Modeling the electrical and thermal response of superconducting nanowire single-photon detectors. IEEE Trans. Appl. Supercond. **17**, 581–585 (2007)

24. M.A. Wolff, S. Vogel, L. Splitthoff, C. Schuck, Superconducting nanowire single-photon detectors integrated with tantalum pentoxide waveguides. Sci. Rep. (2020). https://doi.org/10.1038/s41598-020-74426-w

25. H.B. Zhang, J.K. Liu, J.H. Guo, L. Xiao, J. Xie, Photon energy-dependent timing jitter and spectrum resolution research based on time-resolved SNSPDs. Opt. Express **28**, 16696–16707 (2020)

26. P. Ravindran, R.S. Cheng, H. Tang, J.C. Bardin, Active quenching of superconducting nanowire single photon detectors. Opt. Express **28**, 4099–4114 (2020)

27. X. Tao et al., Characterize the speed of a photon-number-resolving superconducting nanowire detector. IEEE Photonics J. **12**, 1–8 (2020)

28. F. Garzetti et al., Assessment of the bundle SNSPD plus FPGA-based TDC for high-performance time measurements. IEEE Access **10**, 127894–127910 (2022)

29. F. Beutel, T. Grottke, M.A. Wolff, C. Schuck, W.H.P. Pernice, Cryo-compatible opto-mechanical low-voltage phase-modulator integrated with superconducting single-photon detectors. Opt. Express **30**, 30066–30074 (2022)

30. S. Miyajima et al., Single-flux-quantum signal processors monolithically integrated with a superconducting nanostrip single-photon detector array. Appl. Phys. Lett. (2023). https://doi.org/10.1063/5.0144808

31. M. Yabuno, S. Miyajima, S. Miki, H. Terai, Scalable implementation of a superconducting nanowire single-photon detector array with a superconducting digital signal processor. Opt. Express **28**, 12047–12057 (2020)

32. C. Joshi et al., Picosecond-resolution single-photon time lens for temporal mode quantum processing. Optica **9**, 364–373 (2022)

33. H. Wu, C. Gu, Y. Cheng, X. Hu, Vortex-crossing-induced timing jitter of superconducting nanowire single-photon detectors. Appl. Phys. Lett. (2017). https://doi.org/10.1063/1.4997930

34. I. Esmaeil Zadeh et al., Efficient single-photon detection with 7.7 ps time resolution for photon-correlation measurements. ACS Photonics **7**, 1780–1787 (2020)

35. B. Korzh et al., Demonstration of sub-3 ps temporal resolution with a superconducting nanowire single-photon detector. Nat. Photonics **14**, 250–255 (2020)

36. M. Sidorova et al., Physical mechanisms of timing jitter in photon detection by current-carrying superconducting nanowires. Phys. Rev. B (2017). https://doi.org/10.1103/PhysRevB.96.184504

37. M.J. Stevens et al., Infrared wavelength-dependent optical characterization of NbN nanowire superconducting single-photon detectors. J. Mod. Opt. **56**, 358–363 (2009)

38. J. Zhang et al., Time delay of resistive-state formation in superconducting stripes excited by single optical photons. Phys. Rev. B (2003). https://doi.org/10.1103/PhysRevB.67.132508

39. J.P. Allmaras, A.G. Kozorezov, B.A. Korzh, K.K. Berggren, M.D. Shaw, Intrinsic timing jitter and latency in superconducting nanowire single-photon detectors. Phys. Rev. Appl. (2019). https://doi.org/10.1103/PhysRevApplied.11.034062

40. D.Y. Vodolazov, Single-photon detection by a dirty current-carrying superconducting strip based on the kinetic-equation approach. Phys. Rev. Appl. (2017). https://doi.org/10.1103/PhysRevApplied.7.034014

41. N. Zen et al., 1 mm ultrafast superconducting stripline molecule detector. Appl. Phys. Lett. **95**, 172508 (2009)

42. A. Casaburi et al., Thicker, more efficient superconducting stripline detectors for high throughput macromolecules analysis. Appl. Phys. Lett. **98**, 023702 (2011)

43. K. Suzuki et al., Hot-spot detection model in superconducting nano-stripline detector for keV ions. Appl. Phys. Express **4**, 083101 (2011)

44. D. Perez de Lara et al., Feasibility investigation of NbN nanowires as detector in time-of-flight mass spectrometers for macromolecules of interest in biology (proteins). J. Low Temp. Phys. **151**, 771–776 (2008)

45. X. Zhang, Q. Wang, A. Schilling, Superconducting single X-ray photon detector based on W0.8Si0.2. AIP Adv. **10**(1063/1), 4967278 (2016)

46. Zhang, H.B. *et al.* in Conference on Advanced Sensor Systems and Applications X, Vol. 11554 (Electr Network; 2020)

47. S.Y. Guo et al., High-timing-precision detection of single X-ray photons by superconducting nanowires. Nat. Sci. Rev. (2023). https://doi.org/10.1093/nsr/nwad102

48. A. Branny et al., X-Ray induced secondary particle counting with thin NbTiN nanowire superconducting detector. IEEE Trans. Appl. Supercond. **31**, 1–5 (2021)

49. L. Chen et al., Mid-infrared laser-induced fluorescence with nanosecond time resolution using a superconducting nanowire single-photon detector: new technology for molecular science. Acc. Chem. Res. **50**, 1400–1409 (2017)

50. J. Chang et al., Efficient mid-infrared single-photon detection using superconducting NbTiN nanowires with high time resolution in a Gifford-McMahon cryocooler. Photonics Res. **10**, 1063–1070 (2022)

51. R. Sobolewski, A. Verevkin, G.N. Gol'tsman, A. Lipatov, K. Wilsher, Ultrafast superconducting single-photon optical detectors and their applications. IEEE Trans. Appl. Supercond. **13**, 1151–1157 (2003)

52. A. Korneev et al., Sensitivity and gigahertz counting performance of NbN superconducting single-photon detectors. Appl. Phys. Lett. **84**, 5338–5340 (2004)

53. I.E. Zadeh et al., Single-photon detectors combining high efficiency, high detection rates, and ultra-high timing resolution. APL Photonics (2017). https://doi.org/10.1063/1.5000001

54. R.Y. Ma et al., Single photon detection performance of highly disordered NbTiN thin films. J. Phys. Commun. **7**, 055006 (2023)

55. C. Cirillo et al., Superconducting nanowire single photon detectors based on disordered NbRe films. Appl. Phys. Lett. (2020). https://doi.org/10.1063/5.0021487

56. A.J. Annunziata, Single-photon detection, kinetic inductance, and non-equilibrium dynamics in niobium and niobium nitride Superconducting Nanowires. *Ph.D. thesis* (2010)

57. M. Caloz et al., High-detection efficiency and low-timing jitter with amorphous superconducting nanowire single-photon detectors. Appl. Phys. Lett. **112**, 061103 (2018)

58. M. Caloz et al., Intrinsically-limited timing jitter in molybdenum silicide superconducting nanowire single-photon detectors. J. Appl. Phys. (2019). https://doi.org/10.1063/1.5113748

59. V.B. Verma et al., Superconducting nanowire single photon detectors fabricated from an amorphous Mo0.75Ge0.25 thin film. Appl. Phys. Lett. (2014). https://doi.org/10.1063/1.4890277

60. A. Kumar et al., Ultrafast low-jitter optical response in high-temperature superconducting microwires. Appl. Phys. Lett. (2023). https://doi.org/10.1063/5.0150805

61. K. Likharev, Superconducting weak links. Rev. Mod. Phys. **51**, 101–159 (1979)

62. W.J. Skocpol, M.R. Beasley, M. Tinkham, Self-heating hotspots in superconducting thin-film microbridges. J. Appl. Phys. **45**, 4054–4066 (1974)

63. N. Giordano, Evidence for macroscopic quantum tunneling in one-dimensional superconductors. Phys. Rev. Lett. **61**, 2137–2140 (1988)

64. A. Engel et al., Temperature- and field-dependence of critical currents in NbN microbridges. J. Phys. Conf. Ser. **97**, 012152 (2008)

65. C. Delacour, B. Pannetier, J.-C. Villegier, V. Bouchiat, Quantum and thermal phase slips in superconducting niobium nitride (NbN) ultrathin crystalline nanowire: application to single photon detection. Nano Lett. **12**, 3501–3506 (2012)

66. D. Henrich et al., Broadening of hot-spot response spectrum of superconducting NbN nanowire single-photon detector with reduced nitrogen content. J. Appl. Phys. (2012). https://doi.org/10.1063/1.4757625

67. I. Charaev et al., Current dependence of the hot-spot response spectrum of superconducting single-photon detectors with different layouts. Supercond. Sci. Technol. **30**, 025016 (2016)

68. K. Ilin et al., Current-induced critical state in NbN thin-film structures. J. Low Temp. Phys. **151**, 585–590 (2008)

69. J.K.W. Yang et al., Suppressed critical current in superconducting nanowire single-photon detectors with high fill-factors. IEEE Trans. Appl. Supercond. **19**, 318–322 (2009)

70. R. Hortensius, E. Driessen, T.M. Klapwijk, K. Berggren, J. Clem, Critical-current reduction in thin superconducting wires due to current crowding. Appl. Phys. Lett. (2012). https://doi.org/10.1063/1.4711217

71. J.R. Clem, K.K. Berggren, Geometry-dependent critical currents in superconducting nanocircuits. Phys. Rev. B (2011). https://doi.org/10.1103/PhysRevB.84.174510

72. K. Il'in, M. Siegel, A. Semenov, A. Engel, H.W. Hübers, Critical current of Nb and NbN thin-film structures: the cross-section dependence. Phys. Stat. Sol (c) **2**, 1680–1687 (2005)

73. A.J. Kerman et al., Constriction-limited detection efficiency of superconducting nanowire single-photon detectors. Appl. Phys. Lett. (2007). https://doi.org/10.1063/1.2696926

74. A.N. Zotova, The contribution of bends and constrictions of a superconducting film to the photon detection by a single-photon superconducting detector. J. Exp. Theor. Phys. **122**, 818–822 (2016)

75. R. Gaudio, T. Hoog et al., Inhomogeneous critical current in nanowire superconducting single-photon detectors. Appl. Phys. Lett. **105**, 222602 (2014)

76. H.L. Hortensius, E.F.C. Driessen, T.M. Klapwijk, Possible indications of electronic inhomogeneities in superconducting nanowire detectors. IEEE Trans. Appl. Supercond. **23**, 2200705 (2013)

77. J.A. O'Connor et al., Spatial dependence of output pulse delay in a niobium nitride nanowire superconducting single-photon detector. Appl. Phys. Lett. (2011). https://doi.org/10.1063/1.3581054

78. Y. Cheng, C. Gu, X. Hu, Inhomogeneity-induced timing jitter of superconducting nanowire single-photon detectors. Appl. Phys. Lett. (2017). https://doi.org/10.1063/1.4985226

79. A.G. Kozorezov et al., Fano fluctuations in superconducting-nanowire single-photon detectors. Phys. Rev. B (2017). https://doi.org/10.1103/PhysRevB.96.054507

80. M. Colangelo et al., Impedance-matched differential superconducting nanowire detectors. Phys. Rev. Appl. (2023). https://doi.org/10.1103/PhysRevApplied.19.044093

81. M. Sidorova et al., Timing jitter in photon detection by straight superconducting nanowires: effect of magnetic field and photon flux. Phys. Rev. B (2018). https://doi.org/10.1103/PhysRevB.98.134504

82. G.R. Berdiyorov, M.V. Milosevic, F.M. Peeters, Spatially dependent sensitivity of superconducting meanders as

83. single-photon detectors. Appl. Phys. Lett. (2012). https://doi.org/10.1063/1.4731627

83. A. Pearlman et al., Gigahertz counting rates of NbN single-photon detectors for quantum communications. IEEE Trans. Appl. Supercond. **15**, 579–582 (2005)

84. A. Dane et al., Self-heating hotspots in superconducting nanowires cooled by phonon black-body radiation. Nat. Commun. (2022). https://doi.org/10.1038/s41467-022-32719-w

85. B. Mazin, P. Day, H. LeDuc, A. Vayonakis, J. Zmuidzinas, Superconducting kinetic inductance photon detectors. InHighly Innov. Space Telesc. Concepts **4849**, 283–293 (2002)

86. A.G. Kozorezov, J.K. Wigmore, D. Martin, P. Verhoeve, A. Peacock, Resolution limitation in superconducting transition edge photon detectors due to downconversion phonon noise. Appl. Phys. Lett. (2006). https://doi.org/10.1063/1.2397016

87. D.D.E. Martin et al., Resolution limitation due to phonon losses in superconducting tunnel junctions. Appl. Phys. Lett. (2006). https://doi.org/10.1063/1.2187444

88. M. Caloz et al., Optically probing the detection mechanism in a molybdenum silicide superconducting nanowire single-photon detector. Appl. Phys. Lett. (2017). https://doi.org/10.1063/1.4977034

89. L.-P. Yang, H. Tang, Z. Jacob, Concept of quantum timing jitter and non-Markovian limits in single-photon detection. Phys. Rev. A (2018). https://doi.org/10.1103/PhysRevA.97.013833

90. S. Jahani et al., Probabilistic vortex crossing criterion for superconducting nanowire single-photon detectors. J. Appl. Phys. **127**, 143101 (2020)

91. R. Flaschmann et al., The dependence of timing jitter of superconducting nanowire single-photon detectors on the multi-layer sample design and slew rate. Nanoscale **15**, 1086–1091 (2023)

92. T.M. Rambo, *et al.* In Conference on Quantum Optics and Photon Counting, Vol. 12570 (Prague, CZECH REPUBLIC; 2023)

93. I. Craiciu et al., High-speed detection of 1550 nm single photons with superconducting nanowire detectors. Optica **10**, 183–190 (2023)

94. A. Mueller et al., Time-walk and jitter correction in SNSPDs at high count rates. Appl. Phys. Lett. (2023). https://doi.org/10.1063/5.0129147

95. L. You et al., Jitter analysis of a superconducting nanowire single photon detector. AIP Adv. (2013). https://doi.org/10.1063/1.4817581

96. N. Calandri, Q.-Y. Zhao, D. Zhu, A. Dane, K.K. Berggren, Superconducting nanowire detector jitter limited by detector geometry. Appl. Phys. Lett. (2016). https://doi.org/10.1063/1.4963158

97. J. Wu et al., Improving the timing jitter of a superconducting nanowire single-photon detection system. Appl. Opt. **56**, 2195–2200 (2017)

98. M. Sidorova et al., Intrinsic jitter in photon detection by straight superconducting nanowires. IEEE Trans. Appl. Supercond. **28**, 1–4 (2018)

99. L. Kong et al., Probabilistic energy-to-amplitude mapping in a tapered superconducting nanowire single-photon detector. Nano Lett. **22**, 1587–1594 (2022)

100. P. Haas et al., Spectral sensitivity and spectral resolution of superconducting single-photon detectors. Appl. Supercond., IEEE Trans. **17**, 298–301 (2007)

101. A. Semenov et al., Energy resolution and sensitivity of a superconducting quantum detector. Phys. C **460–462**, 1491–1492 (2007)

102. J. Kitaygorsky et al., HEMT-based readout technique for dark- and photon-count studies in NbN superconducting single-photon detectors. IEEE Trans. Appl. Supercond. **19**, 346–349 (2009)

103. J. Kitaygorsky et al., Amplitude distributions of dark counts and photon counts in NbN superconducting single-photon

detectors integrated with the HEMT readout. Phys. C-Supercond. Appl. **532**, 33–39 (2017)

104. E. Reiger et al., Spectroscopy with nanostructured superconducting single photon detectors. IEEE J. Sel. Top. Quantum Electron. **13**, 934–943 (2007)

105. A.D. Semenov et al., Energy resolution of a superconducting nanowire single-photon detector. J. Low Temp. Phys. **151**, 564–569 (2008)

106. L. Kong et al., Single-detector spectrometer using a superconducting nanowire. Nano Lett. **21**, 9625–9632 (2021)

107. Y. Zhou et al., Response properties of NbN superconductor nanowire for multi-photon. Acta Phys. Sin. **61**, 208501 (2012)

108. M. Bell et al., Photon number-resolved detection with sequentially connected nanowires. IEEE Trans. Appl. Supercond. **17**, 289–292 (2007)

109. K. Ota, *et al.* In 15th International Superconductive Electronics Conference (ISEC) (Nagoya, JAPAN; 2015)

110. C. Wan, Z. Jiang, L. Kang, P.H. Wu, High input impedance cryogenic RF amplifier for series nanowire detector. IEEE Trans. Appl. Supercond. **27**, 1–5 (2017)

111. H. Myoren et al., Readout circuit based on single-flux-quantum logic circuit for photon-number-resolving SNSPD array. IEEE Trans. Appl. Supercond. **28**, 1–4 (2018)

112. H.R. Zhou et al., Photon number resolvability of multi-pixel superconducting nanowire single photon detectors using a single flux quantum circuit. Chin. Phys. B **31**, 057401 (2022)

113. D. Zhu et al., Resolving photon numbers using a superconducting nanowire with impedance-matching taper. Nano Lett. **20**, 3858–3863 (2020)

114. C. Cahall et al., Multi-photon detection using a conventional superconducting nanowire single-photon detector. Optica **4**, 1534–1535 (2017)

115. C. Cahall, *et al.* In Conference on Lasers and Electro-Optics (CLEO) (San Jose, CA; 2018).

116. C.E. Marvinney, *et al.* In Conference on Lasers and Electro-Optics (CLEO) (San Jose, CA; 2020).

117. K.L. Nicolich et al., Universal model for the turn-on dynamics of superconducting nanowire single-photon detectors. Phys. Rev. Appl. (2019). https://doi.org/10.1103/PhysRevApplied.12.034020

118. K.L. Nicolich, *et al.* In Conference on Lasers and Electro-Optics (CLEO) (San Jose, CA; 2018)

119. S. Sempere-Llagostera, G.S. Thekkadath, R.B. Patel, W.S. Kolthammer, I.A. Walmsley, Reducing g((2))(0) of a parametric down-conversion source via photon-number resolution with superconducting nanowire detectors. Opt. Express **30**, 3138–3147 (2022)

120. T. Schapeler, J.P. Hopker, T.J. Bartley, Quantum detector tomography of a high dynamic-range superconducting nanowire single-photon detector. Supercond. Sci. Technol. **34**, 064002 (2021)

121. A.N. Vetlugin, F. Martinelli, S.Y. Dong, C. Soci, Photon number resolution without optical mode multiplication. Nanophotonics **12**, 505–519 (2023)

122. J.W.N. Los, *et al.* (2024)

123. A.E. Lita, D.V. Reddy, V.B. Verma, R.P. Mirin, S.W. Nam, Development of superconducting single-photon and photon-number resolving detectors for quantum applications. J. Lightwave Technol. **40**, 7578–7597 (2022)

124. S.I. Davis et al., Improved heralded single-photon source with a photon-number-resolving superconducting nanowire detector. Phys. Rev. Appl. (2022). https://doi.org/10.1103/PhysRevApplied.18.064007

125. B. Zhang et al., An all-day lidar for detecting soft targets over 100 km based on superconducting nanowire single-photon detectors. Supercond. Sci. Technol. **34**, 034005 (2021)

126. E. Schmidt et al., Characterization of a photon-number resolving SNSPD using poissonian and sub-poissonian light. IEEE Trans. Appl. Supercond. **29**, 1–5 (2019)

127. X.C. Yan et al., Model of bit error rate for laser communication based on superconducting nanowire single photon detector. Acta Phys. Sin. **66**, 122–237 (2017)

128. F. Mattioli et al., Photon-number-resolving superconducting nanowire detectors. Supercond. Sci. Technol. **28**, 15 (2015)

129. E.A. Dauler et al., Multi-element superconducting nanowire single-photon detector. IEEE Trans. Appl. Supercond. **17**, 279–284 (2007)

130. D.K. Liu et al., Photon-number resolving and distribution verification using a multichannel superconducting nanowire single-photon detection system. J. Opt. Soc. Am. B-Opt. Phys. **31**, 816–820 (2014)

131. J. Huang et al., High speed superconducting nanowire single-photon detector with nine interleaved nanowires. Supercond. Sci. Technol. **31**, 074001 (2018)

132. W.J. Zhang et al., A 16-pixel interleaved superconducting nanowire single-photon detector array with a maximum count rate exceeding 1.5 GHz. IEEE Trans. Appl. Supercond. **29**, 1–4 (2019)

133. N. Lusardi, J.W.N. Los, R.B.M. Gourgues, G. Bulgarini, A. Geraci, Photon counting with photon number resolution through superconducting nanowires coupled to a multi-channel TDC in FPGA. Rev. Sci. Instrum. (2017). https://doi.org/10.1063/1.4977594

134. S. Doerner, A. Kuzmin, S. Wuensch, K. Ilin, M. Siegel, Operation of superconducting nanowire single-photon detectors embedded in lumped-element resonant circuits. IEEE Trans. Appl. Supercond. **26**, 1–5 (2016)

135. S. Doerner et al., Frequency-multiplexed bias and readout of a 16-pixel superconducting nanowire single-photon detector array. Appl. Phys. Lett. (2017). https://doi.org/10.1063/1.4993779

136. S. Doerner, A. Kuzmin, S. Wuensch, I. Charaev, M. Siegel, Operation of multipixel radio-frequency superconducting nanowire single-photon detector arrays. IEEE Trans. Appl. Supercond. **27**, 1–5 (2017)

137. A. Korneev, *et al.* In 8th European Conference on Applied Superconductivity, Vol. 97 (Brussels, BELGIUM; 2007)

138. A. Korneev, *et al.* In 6th International Conference on Photonics, Vol. 7138 (Prague, CZECH REPUBLIC; 2008)

139. G. Goltsman et al., Ultrafast superconducting single-photon detector. J. Mod. Opt. **56**, 1670–1680 (2009)

140. A. Divochiy et al., Superconducting nanowire photon-number-resolving detector at telecommunication wavelengths. Nat. Photonics **2**, 302–306 (2008)

141. F. Marsili, *et al.* In Conference on Lasers and Electro-Optics/Quantum Electronics and Laser Science Conference (CLEO/QELS 2008) 3227-+ (San Jose, CA; 2008)

142. F. Marsili et al., Superconducting parallel nanowire detector with photon number resolving functionality. J. Mod. Opt. **56**, 334–344 (2009)

143. L. Stasi et al., Fast high-efficiency photon-number-resolving parallel superconducting nanowire-photon detector. Phys. Rev. Appl. **19**(6), 064041 (2023)

144. L. Stasi et al., High-efficiency photon-number-resolving detector for improving heralded single-photon sources. Quant. Sci. Technol. **8**(4), 045006 (2023)

145. S. Jahanmirinejad, & A. Fiore, In Conference on Quantum Optics II, Vol. 8440 (Brussels, BELGIUM; 2012)

146. S. Jahanmirinejad et al., Photon-number resolving detector based on a series array of superconducting nanowires. Appl. Phys. Lett. **101**, 072602 (2012)

147. F. Mattioli, *et al.* In 11th European Conference on Applied Superconductivity (EUCAS), Vol. 507 (Genoa, ITALY; 2013)

148. F. Mattioli, *et al.* In 16th Fotonica AEIT Italian Conference on Photonics Technologies (Naples, ITALY; 2014)

149. Z.L. Zhou et al., Superconducting series nanowire detector counting up to twelve photons. Opt. Express **22**, 3475–3489 (2014)

150. X. Tao et al., A high speed and high efficiency superconducting photon number resolving detector. Supercond. Sci. & Technol. **32**, 064002 (2019)

151. R.Y. Xu et al., Experimental demonstration of superconducting series nanowire photon-number-resolving detector at 660 nm wavelength. IEEE Photonics J. **11**, 1–8 (2019)

152. R.S. Cheng et al., Photon-number-resolving detector based on superconducting serial nanowires. IEEE Trans. Appl. Supercond. **23**, 2200309 (2013)

153. G.N. Goltsman, In Conference on Quantum Communications Realized II, Vol. 7236 (San Jose, CA; 2009)

154. E.A. Dauler et al., Photon-number-resolution with sub-30-ps timing using multi-element superconducting nanowire single photon detectors. J. Mod. Opt. **56**, 364–373 (2009)

155. S. Miki, M. Yabuno, T. Yamashita, H. Terai, Stable, high-performance operation of a fiber-coupled superconducting nanowire avalanche photon detector. Opt. Express **25**, 6796–6804 (2017)

156. R. Cheng, M. Poot, X. Guo, L. Fan, H.X. Tang, Large-area superconducting nanowire single-photon detector with double-stage avalanche structure. IEEE Trans. Appl. Supercond. **27**, 1–5 (2017)

157. M. Perrenoud et al., Operation of parallel SNSPDs at high detection rates. Supercond. Sci. Technol. **34**, 024002 (2021)

158. R.S. Cheng et al., A 100-pixel photon-number-resolving detector unveiling photon statistics. Nat. Photonics **17**, 112 (2023)

159. G.V. Resta et al., Gigahertz detection rates and dynamic photon-number resolution with superconducting nanowire arrays. Nano Lett. **23**, 6018–6026 (2023)